Comparison of the performances of handheld and benchtop near infrared spectrometers: Application on the quantification of chemical components in maritime pine (Pinus Pinaster) resin

Morandise Rubini, Lisa Feuillerat, Thomas Cabaret, Léo Leroyer, Luc Leneveu, Bertrand Charrier

HAL Id: hal-03127026
https://univ-pau.hal.science/hal-03127026

Submitted on 22 Aug 2022

Title: Comparison of the performances of handheld and benchtop near infrared spectrometers:

application on the quantification of chemical components in maritime pine (*Pinus Pinaster*)

resin

Morandise Rubini [a*]; Lisa Feuillerat [a]; Thomas Cabaret [a]; Léo Leroyer [a]; Luc Leneveu [b];

Bertrand Charrier [a]

[a] CNRS/Université de Pau des Pays de l'Adour, Institut des sciences analytiques et de physico-

chimie pour l'environnement et les matériaux, Xylomat, UMR5254, 40004, Mont de Marsan,

France

[b] Biogemme - Holiste, 40600, Biscarrosse, France

* Corresponding authors

Corresponding authors e-mail address: morandise.rubini@univ-pau.fr

1 Introduction

Maritime pine (*Pinus pinaster*) tapping (resin collection) was a prominent activity in France from the 19th century until the 1970's [1]. Maritime pine covers in the Southwest of France more than one million hectares [2]. After the 1970s, tapping drastically declines because its lost its profitability, mainly because to the growth of the Chinese market [3,4]. Recently, tapping reemerged [5] with new, mechanized tapping techniques, in a context with concerns about harvesting in sustainable and environmentally friendly conditions [6].

Closed cup tapping is one of these techniques. The first works are related to (C. Courau, 1996) [7]. Closed cup tapping became increasingly popular in France and is currently being improved [8]. Briefly described, a superficial incision using a circular saw removes a section of the bark and of the secondary phloem, where the resin is formed [9]. Then, a stimulant paste composed of natural acids is applied to activate resin exudation. Finally, a bottleneck guides the drained resin into an airtight sealed plastic bag, which protects the resin from impurities such as insects, sand, plant debris or rainwater, and limits evaporation.

Resin exudates abundantly [10] as a complex mixture of a volatile fraction (turpentine) and a nonvolatile fraction (rosin) [11,12]. Turpentine consists of a few unsaturated hydrocarbon monoterpenes, with smaller amounts of other monoterpenes [13,14]. Rosin is mainly composed of diterpenic monocarboxylic acids, plus neutral components [15–17]. The various components can be analyzed quantitatively using gas chromatography [18–21] and or liquid chromatography [22,23]. These methods are used for quality control and to select higher quality resin, but they are time-consuming and hard to use on-site. Considering this, the present study looks for alternative analytical methods, including Near infrared (NIR) spectroscopy in combination with chemometrics [24,25].

NIR spectroscopy is a non-destructive, reliable, and rapid tool for quantification, and can be applied on portable devices [26]. Indeed, low cost handheld near-infrared spectrometer, such

26 as *SCiO* (*Consumer Physics*, Israel), has been reported in the literature as a reliable and

27 inexpensive technology, which facilitates its use on an industrial scale [27–32]. The objective

28 of this study is to assess the potential of *SCiO* as a direct and rapid analysis tool for the

29 quantification of the main chemical components of *Pinus pinaster* resin with chemometric

30 processing.

31 Partial Least Squares (PLS) regression was used to develop quantitative predictive models.

32 Those models were optimized various different spectral preprocessing methods. Then, the

33 performance of *SCiO* was compared to the baseline of a benchtop spectrometer.

34 **2   Materials and methods**

35   *2.1   Sample collection and conservation*

36 One hundred and twenty-five samples of maritime pine (*Pinus pinaster*) resin were harvested

37 in Biscarrosse (Landes, France) during the summer of 2018. They were collected by tapping

38 one hundred and twenty-five fifty years old trees using a closed cup tapping technique

39 patented by (L. Leneveu, 2002) [8]. Briefly described, the method consisted in having the

40 resin flow into a sealed plastic bag made of an ethylene vinyl alcohol (EVOH) inner film (70

41 μm thick) and a low-density polyethylene (LDPE) outer film (45 μm thick).

42 Once, the samples were stored in a box kept away from light and heat in order avoid chemical

43 alteration.

44   *2.2   Reference methods*

45   *2.2.1   Proportion of turpentine fraction in Pinus pinaster resin (% turpentine)*
46   *using a ventilated oven*

47 *For convenience, the relative proportion of turpentine and rosin fractions is designated here*

48 *collectively as the "Proportion of turpentine fraction".*

2

49 The proportion of turpentine fraction in maritime pine (*Pinus pinaster*) resin (*% turpentine*)

50 was quantified using a ventilated oven.

51 The *% turpentine* was an important data for this study, because, the chemical composition

52 was determined with two different analytical instruments, and the chemical composition

53 pertains respectively to each fraction. Therefore, *% turpentine* is an indicator of the actual

54 amount of the chemical components in each of the fractions.

55 Briefly, 2 g of resin were poured in a aluminium cup. The weight difference before and after

56 drying was used to determine *% turpentine*. Each sample was placed in a ventilated oven at a

57 temperature close to the boiling point of monoterpenes, for a duration sufficient to provoke its

58 evaporation. Specifically, the samples were placed at 150 °C for 30 min in the ventilated

59 oven.

60   *2.2.2 Chemical composition of the turpentine as determined via Gas*

61   *Chromatography coupled to a Flame Ionization Detector (GC–FID)*

62   *analysis and sample preparation*

63 The chemical composition of the turpentine fraction from maritime pine (*Pinus pinaster*) resin

64 was quantified using a Perkim-Elmer Clarus 500 gas chromatograph (GC) coupled to a Flame

65 Ionization Detector (FID), and a Perkim-Elmer Elite-5MS capillary column (30 m x 0,25 mm

66 x 0,5 μm film thickness).

67 To prepare the samples, the plastic bag containing the resin was homogenized manually for

68 several minutes until the turpentine and rosin were completely mixed. Then, 10 mL of the

69 resin were poured in a cylindrical glass vial (h = 50 mm, outer diameter = 22 mm). After three

70 days, 0.5 mL of supernatant containing turpentine was diluted with 1.5 ml of hexane, which

71 was, in turn, stirred in an ultrasonic bath for 1 min, then filtered through a 0.2 μm nylon filter

72 before injecting. 1 μL of this solution.

73 The experimental conditions developed in the laboratory were as follow: both injector and

74 detector temperatures were set at 290 °C; oven temperature program, 50 to 150 °C (2 °C/min),

75 then 150 to 320 °C (10 °C/min); hydrogen was used as carrier gas. The first ramp was used to

76 elute the volatile components of the turpentine, the second ramp was used to clean the

77 column.

78 Between each sample injection, two flash cleaning programs with acetone and hexane were

79 applied to remove any residue (50 to 250 °C (15 °C/min)).

80 For the identification of the components of the turpentine fraction, Kovats's linear retention

81 index was calculated from the injection of a homologous series of hydrocarbons (C8 – C20)

82 and compared with literature data [33], in accordance with ASTM D6730 [34]. For the

83 quantitative analysis, the respective rates were expressed as percentages.

84   *2.2.3   Chemical composition of the rosin fraction determined via High-*

85   *Performance Liquid Chromatography coupled to Diode Array*

86   *Detectors (HPLC-DAD) and sample preparation*

87 The chemical composition of the rosin fraction from maritime pine (*Pinus pinaster*) resin was

88 quantified using High-Performance Liquid Chromatography coupled to a Diode Array

89 Detector (HPLC-DAD). A methodology similar to the ones already reported was used

90 [35,36]. Briefly, the plastic bag containing the resin was homogenized manually for several

91 minutes until the turpentine and rosin were completely mixed. Then, 1 % w/v of the sample

92 was diluted in Methanol. 10 µL of this solution was injected in a Thermo Scientific Ultimate

93 3000 chromatographic unit equipped with a Thermo Scientific LC Acclaim PolarAdvantage II

94 C18 column (5 µm, 150 x 4.6 mm), and a Diode Array Detector. The separation was carried

95 out at 20 °C with a binary gradient mixture of solvent A (methanol + 1.0 % formic acid) and

96 solvent B (water + 1.0 % formic acid). A flow rate of 300 µl/min was used with a gradient

4

97   program as follow: 0-2 min (60 % of A); 2-17 min. (60-80 % of A); 17-34 min. (80 % of A);

98   34-48 min. (80-100 % of A); 48-67 min. (100 % of A); equilibrated (60 % of A).

99   The methodologies described by (Lee et al., 1997; Kersten et al., 2006) [22,23] were used for

100   identification and quantification of the chemical components of the rosin fraction.

101   *2.3   Near infrared (NIR) acquisition*

102   Near infrared (NIR) acquisition was performed using a benchtop spectrometer and a handheld

103   spectrometer, respectively, *MultiPurpose Analyzer I* (*Bruker*, USA) and *SCiO* (*Consumer*

104   *Physics*, Israel).

105   *MultiPurpose Analyzer I* is a Fourier transform near infrared (FT-NIR) spectrometer

106   implemented with an integrating sphere. The spectral range of acquisition was between

107   12,500 to 4,166 cm^{-1} (780 to 2400 *nm*) with a nominal resolution of 8 cm^{-1}. For the spectral

108   acquisition, resin was poured in a cylindrical glass vial (h = 50 mm, outer diameter = 22 mm),

109   and placed over the sphere window, with an average of 16 scans for each spectrum.

110   *The SCiO* handheld spectrometer [37] operated in a spectral range between 13,514 to 9,346

111   cm^{-1} (740 to 1070 *nm*) with values every 1 nm and an optical resolution of 30 nm [38]. The

112   resin samples were scanned directly through the sealed plastic bag using an accessory

113   provided by *Consumer Physics* to avoid ambient light interference, and also to ensure a

114   constant distance of 10 mm between the light source and the sample. For each sealed plastic

115   bag, the spectrum was calculated as the median of six measurements.

116   As the *SCiO* is a cloud-based device, *Consumer Physics* proposes a commercial online

117   toolkit, which is required for spectra acquisition and download them. This online toolkit is

118   also useful to create online mathematical models, which can be implemented in a mobile

119   application using the *Software Development Kit* provided by *Consumer Physics*. Yet, this

120   application was not used in the present study.

121   *2.4   Multivariate Data Analysis*

122   Fig. 1 details the process used during the Multivariate Data Analysis. The same methodology

123   was applied on both spectrometers, in order to compare their quantitative predictive ability.

124   *2.4.1   Preprocessing*

125   During spectral data acquisition, scattering of photons leads to many physical phenomena

126   (lengthening of the optical path, noise) that need to be corrected with spectra preprocessing

127   algorithms [39] to limit the influence of physical phenomena on the relevant properties [40].

128   Such effects include baseline drift, nonlinearity, curvilinearity, additive and multiplicative

129   effects, and irrelevant variations in the spectra [40]. Thus, several preprocessing techniques

130   were applied in order to increase the accuracy of the predictive models: Standard Normal

131   Variate (SNV), Detrend (DT2), combination of SNV and DT2 [41], Multiplicative Scatter

132   Correction (MSC) [42], and Savitzky-Golay's first and second derivatives [43].

133   *2.4.2   Subset Selection*

134   Subset selection algorithms were used to extract calibration and independent validation

135   subsets   from   a   dataset   [44].   The   DUPLEX   algorithm   [45]   promotes   sample

136   representativeness, ensuring that the selected spectra are uniformly distributed in the

137   multidimensional data space and that the dependent variable has the same statistics

138   characteristics (mean, variance, range, etc.).

139   In the first step, the two spectra most distant from each other are selected and placed in the

140   calibration subset. On the remaining spectra, the following pair of spectra most distant from

141   each other are selected for the validation subset. By alternating subsets, the procedure

142   continues to select a single spectrum for each subset of data. The selected spectrum is the one

143   farthest from the spectra already selected within the subset. Once the required number of

144 samples is reached in the validation subsets, the remaining samples are placed in the

145 calibration subset.

146 With this procedure, the dataset was split as follow: 70 % in the calibration subset, and 30%

147 in the validation subset.

148 ### 2.4.3   Modelling Phase

149 Partial Least Squares (PLS) regression with Nonlinear Iterative Partial Least Squares

150 (NIPALS) algorithm is the favorite for regression in NIR applications, because of its ability to

151 analyze high-dimensional and multi-collinear data [46,47]. Its purpose is to use independent

152 variables (X) to predict a dependent variable (y): the spectra (X) are used to predict the

153 analytical reference values (y). To achieve this goal, it will attempt to meet three objectives:

154 (i) explain X; (ii) explain y; (iii) find relationships between X and y. Nonlinear Iterative

155 Partial Least Squares (NIPALS) has been used as algorithm to perform PLS.

156 In order to evaluate the quantitative predictive ability of Partial Least Squares (PLS) models,

157 several merit scores were computed. The coefficient of determination gave a measure of

158 linearity of the prediction based either on the calibration subset (R^2_{Cal}; R^2_{CV}), or on the

159 validation subset (R^2_{Val}). Root Mean Square Error of Calibration, Cross-Validation and

160 Prediction (respectively, RMSEC, RMSECV and RMSEP) were used to measure the accuracy

161 of the prediction calculated on both the calibration and validation subsets.

162 Another figure of merit, the Ratio of standard error of Performance to standard Deviation

163 (RPD), was computed to classify the applicability of the models. According to (Williams,

164 2014) [48], higher RPD values were associated with better quantitative prediction.

165 General rules emerge to classify the applicability of the models: with $2.5 \leq$ RPD < 3.0, the

166 quantitative model makes approximate quantitative predictions (screening); with $3.0 \leq$ RPD $<$

167 3.5, good quantitative predictions (quality control); for $3.5 \leq$ RPD < 4.1, very good

168 quantitative predictions (process control); and RPD ≥ 4.1 indicates an excellent quantitative

169 predictive model.

170 *2.4.4 Software*

171 Chemometric models construction was carried out using Matlab 2019a (Mathworks Inc.,

172 USA) with the SAISIR toolbox [49], and all the scripts were designed in-house.

173 **3 Results and discussion**

174 *3.1 Chemical composition and % turpentine of maritime pine (Pinus pinaster) resin*

175 Table 1 list the values of the studied parameters of maritime pine (*Pinus pinaster*) samples:

176 main chemical components of the turpentine and rosin fractions, and proportion of the

177 turpentine fraction.

178 Concerning the turpentine fraction, the results obtained via GC-FID showed that the analyzed

179 turpentine of *Pinus pinaster* is mainly composed of unsaturated hydrocarbon monoterpenes,

180 above all α-pinene and β-pinene: the α-pinene content was 66.2 ± 9.0 % and the β-pinene

181 content was 18.5 ± 8.5 %. (Ghanmi et al., 2005) [13], comparing the turpentine content of

182 maritime pine (*Pinus pinaster*) and of Aleppo pine (*Pinus halepensis*) from Morocco, report

183 similar composition values for α-pinene and β-pinene as main components of turpentine: 78.7

184 % for α-pinene, and 7.3 % for β-pinene.

185 Concerning the rosin fraction, the results from HPLC-DAD show that the analyzed rosin of

186 *Pinus pinaster* is mainly composed of diterpenic monocarboxylic acids, such as levopimaric

187 acid, with a content of 62.1 ± 5.9 %. (Arrabal et al., 2005) [50] monitored the oleoresin

188 chemical composition of 150 Spanish *Pinus pinaster* trees aged of 33 years old, from thirty

189 sites. Authors reported similar composition values with levopimaric acid as the main

190 constituent ranging from 41.7 to 45.3 %.

191   The turpentine content (*% turpentine*) was 34.3 ± 6.6 %, also in agreement with the literature:

192   (Arrabal et al., 2005) [50] found *% turpentine* values ranging from 27.7 to 30.3 %.

193   *3.2   NIR spectra*

194   As reminded by (Y. Ozaki, 2012) [51], near infrared can be divided in three regions: region I

195   (800 – 1200 *nm*; 12500 – 8500 cm^{-1}), region II (1200 – 1800 *nm*; 8500 – 5500 cm^{-1}) and

196   region III (1800 – 2500 *nm*; 5500 – 4000 cm^{-1}). Those regions have specific spectral

197   features, covering mainly electronic transitions, overtones and combination bands [52].

198   The benchtop *MPA I* spectrometer covers the 12,500 - 4,166 cm^{-1} range (780 to 2400 *nm*),

199   which roughly corresponds to all these three regions. Along the spectra acquired with the

200   *MPA I*, the *CH* first overtone, third overtone, deformation band and combination band; *OH*

201   second overtone and $C = 0$ first and fourth overtone are observed.

202   The handheld *SCiO* spectrometer covers a narrow range from 13,514 to 9346 cm^{-1} (740 to

203   1070 *nm*), which covers the first region (Region I), also called "*near infrared*", where *CH*

204   third overtone and *OH* second overtone are observed. In fact, the *SCiO's* capacity in the

205   visible domain and the NIR domain are limited [32]. From this information, it is assumed that

206   *MPA I* and *SCiO* spectrometers can consistently detect the same vibrational bands at different

207   overtones.

208   Table 2 reports the vibrational bands of *Pinus pinaster* resin. The table was drafted based on

209   the chemical structure of its major components, the spectra shapes, and the literature [53,54].

210   *3.3   Modelling Phase*

211   Statistics of Partial Least Squares (PLS) regression are presented in Table 3.

212   PLS regression was applied on calibration subsets to develop quantitative predictive models.

213   In PLS modeling, Latent Variables (LVs) were calculated and considered as new eigenvectors

214 to reduce the dimensionality and compress the original spectral data. The number of LVs was

215 determined as the one that provided the lowest RMSECV using a leave-one-out cross-

216 validation. Once developed, the model was applied to validation subsets, which had not been

217 used during the calibration procedures. Then, the predictive ability of each model was

218 assessed by external validation on the validation subsets.

219 As a rule, a good model should have higher R_{Cal}^2, R_{CV}^2, R_{Val}^2 and RPD values, and lower

220 RMSEC, RMSECV and RMSEP. Here, the quantitative predictive ability of the model was

221 selected based on highest RPD values.

222 *3.3.1   Benchtop spectrometer: MultiPurpose Analyzer I (Bruker, USA)*

223 Figure 2 (a) shows the raw spectra acquired with the *MultiPurpose Analyzer I*. Figure 2 (b to

224 g) shows the preprocessed spectra. The raw and preprocessed spectra highlight many

225 vibrational bands, which contain all the information needed for the modelling phase.

226 As seen in Table 3, all the parameters values of the coefficients of determination calculated

227 between reference and predicted data on either calibration or validation subsets are excellent

228 (R_{Cal}^2 > 0.8; R_{CV}^2 >0.8; R_{Val}^2 > 0.8). In this case, PLS regression models predictions are well

229 correlated to the references ones. RMSEC, RMSECV and RMSEP values are low in

230 accordance with the reference data. In addition, they are close, which shows that the PLS

231 regression models are robust. RPD statistics give poorest performance with PLS regression

232 models computed without preprocessing (raw data). This means that spectral preprocessing is

233 mandatory to improve the predictive ability of all models. Concerning the RPD values, all

234 parameters are classified in two groups. In the first group, RPD ≥ 4.1, indicating excellent

235 quantitative predictive models for α-pinene, β-pinene, and abietic and neoabietic acids. In the

236 second group, the RPD ranges from 3.5 to 4.1, indicating very good quantitative predictions,

237 for levopimaric acid and *% turpentine.*

10

238 Concerning the preprocessing, Detrend (DT2) gives better predictive ability for a mixture of

239 abietic and neoabietic acids (RPD = 4.0); Savitzky–Golay first derivatives (SG1) give better

240 predictive ability for α-pinene (RPD = 4.7) and levopimaric acid (RPD = 4.0); Savitzky–

241 Golay second derivatives (SG2) give better predictive ability for β-pinene (RPD = 5.0) and *%*

242 *turpentine* (RPD = 3.5).

243 *3.3.2   Handheld spectrometer: SCiO (Consumer Physics, Israel)*

244 Figure 3 (a) shows the raw spectra acquired with the *SCiO*. The raw spectra seem flat and did

245 not exhibit any characteristic vibrational bands except for *OH* at 957 *nm* (10,449 cm^{-1}). This

246 is seemingly due to physical phenomena, such as scattering effects and overlapping signals

247 [55,56].

248 In practice, *SCiO* lacks repeatability and reproducibility. For example, the same sample area

249 can be scanned (without touching or moving the device) several times, causing intensity shift.

250 (Subedi *et al.*, 2020) [38] is cited as a first attempt to test the repeatability of *SCiO*, and two

251 other spectrometers: *MicroNIR* (*Viavi*, USA) and *F750* (*Felix Instruments*, USA). There the

252 authors expressed the repeatability as the standard deviation of absorbance of the highest

253 signal across the wavelength range monitored. Standard deviation was computed on 20

254 repeated measures of a PTFE reference material. Standard deviation was 0.04, 0.22 and

255 0.40 m Absorbance units for the *F750*, *MicroNIR* and *SCiO* spectrometers respectively. The

256 values obtained with the *SCiO* were much higher than with the others two spectrometers. It is

257 thus necessary, for each sample, to acquire several spectra, and to use a statistical method

258 (*mean*, *median*) in order to have a representative spectrum, and also, to apply preprocessing

259 algorithms. Once the spectra are preprocessed, vibrational bands are highlighted (Figure 3: b -

260 g).

261 Similarly, with the PLS regression models developed for the benchtop spectrometer for all

262 parameters, the values of coefficients of determination (R^2_{Cal}; R^2_{CV}; R^2_{Val}) show good

263 agreement between prediction and reference values. RMSEC, RMSECV and RMSEP values

264 were higher than those obtained with the benchtop device, and show some discrepancy,

265 suggesting that PLS regression models cannot be as robust as with the benchtop device.

266 Looking at RPD statistics, spectral preprocessing is also required to improve the predictive

267 ability of all models. As shown in Table 3, the five parameters can be classified into two

268 groups. In the first group, the RPD ranges from 3.0 to 3.5, which indicate some good

269 quantitative predictive ability for quality control. This group includes all major components of

270 the resin, such as α-pinene, and levopimaric, abietic and neoabietic acids. In the second group,

271 the RPD ranged between 2.5 and 3.0, i.e. β-pinene and *% turpentine* were less correctly

272 predicted.

273 Concerning the preprocessing, Detrend (DT2) gives better predictive ability for the mixture of

274 abietic and neoabietic acids (RPD = 3.01). Combination of Standard Normal Variate and

275 Detrend (SNV + DT2) give better predictive ability for *% turpentine* (RPD = 3.03).

276 Multiplicative Scatter Correction (MSC) gives better predictive ability for levopimaric acid

277 (RPD = 3.09). Savitzky–Golay second derivatives (SG2) give better predictive ability for α-

278 pinene (RPD = 3.16) and β-pinene (RPD = 2.82).

279 **4   Conclusion**

280 The *SCiO* handheld NIR spectrometer was studied as a potential tool to quantify the chemical

281 components of maritime pine (*Pinus pinaster*) resin, in view of its use as a quality control tool

282 for the tapping industry.

283 This study looked at the performance of the handheld *SCiO* spectrometer in comparison with

284 a benchtop *MPA I* spectrometer, and evaluated the performance based on statistical

285 parameters.

286 Although, *SCiO* and *MPA I* work in different NIR regions, PLS regression models can be

287 used to quantify major resin components, such as, α-pinene, β-pinene, levopimaric, abietic

288 and neoabietic acids, and *% turpentine*. Results shown that spectral preprocessing is

289 mandatory to increase the predictive ability of the PLS regression models.

290 Considering the selected PLS models: the coefficients of determination (R^2_{Cal}; R^2_{CV}; R^2_{Val})

291 show good agreement between prediction and reference values for both, *SCiO* and *MPA I*

292 spectrometers with values higher than 0.8; RMSEC, RMSECV and RMSEP values were

293 higher for the *SCiO* compared to the *MPA I*, and they also show some discrepancy, suggesting

294 that PLS regression models for *SCiO* cannot be as robust as *MPA I* models; RPD statistics

295 values were lower for the *SCiO* compared to the *MPA I* – the RPD values for *MPA I* showed

296 an excellent quantitative predictive ability, whereas those for *SCiO* have a good quantitative

297 predictive ability for quality control purposes.

298 Considering the overall instrument parameters (wavelength, resolution, size, cost), the *SCiO*

299 spectrometer showed very good results. Additionally, the *SCiO* is a handheld spectrometer,

300 and can be easily used on-site. Thus, the *SCiO* could be a useful tool to predict main chemical

301 components of maritime pine (*Pinus pinaster*) for quality control in the tapping industry.

302

310 **Declaration of competing interest**

311   The authors declare no actual or potential conflicts of interests.

312 **References**

313 [1] C. Courau, Le gemmage en forêt de Gascogne, 2014.

314 [2] B. Lemoine, N. Decourt, Tables de production pour le pin maritime dans le sud-ouest

315 de la France, Rev. For. Française. (1969) 5. doi:10.4267/2042/20235.

316 [3] J.-C. Bussy, La gemme et les produits résineux en France, Rev. For. Française. 284

317 (1971) 377. doi:10.4267/2042/20503.

318 [4] A. Rodríguez-García, J.A. Martín, R. López, A. Sanz, L. Gil, Effect of four tapping

319 methods on anatomical traits and resin yield in Maritime pine (Pinus pinaster Ait.), Ind.

320 Crops Prod. 86 (2016) 143–154. doi:10.1016/j.indcrop.2016.03.033.

321 [5] M. Castillo Martos, Construir la tecnología: el caso de la resina de pino en Francia,

322 siglos XVIII y XIX, Llull Rev. La Soc. Española Hist. Las Ciencias y Las Técnicas. 26

323 (2003) 1061–1066.

324 [6] C. Courau, La relance du gemmage en forêt de Gascogne, 2009.

325 [7] C. Courau, Procedé de traitement de la résine, dispositif pour la mise en œuvre de ce

326 procedé et colophane obtenue, 1996.

327 [8] L. Leneveu, Procédé pour favoriser l'exsudation de l'oleorésine et composition pour

328 mettre en œuvre ce procédé, 2012.

329 [9] M. Stoffel, M. Klinkmüller, 3D analysis of anatomical reactions in conifers after

330 mechanical wounding: First qualitative insights from X-ray computed tomography,

331 Trees - Struct. Funct. 27 (2013) 1805–1811. doi:10.1007/s00468-013-0900-2.

332 [10] F.A. Neis, F. de Costa, M.R. de Almeida, L.C. Colling, C.F. de Oliveira Junkes, J.P.

333 Fett, A.G. Fett-Neto, Resin exudation profile, chemical composition, and secretory

334 canal characterization in contrasting yield phenotypes of Pinus elliottii Engelm, Ind.

335 Crops Prod. 132 (2019) 76–83. doi:10.1016/j.indcrop.2019.02.013.

336 [11] A.J.D. Silvestre, A. Gandini, Chapter 2 - Terpenes: Major Sources, Properties and

337 Applications, in: Elsevier, 2008: pp. 17–38. doi:https://doi.org/10.1016/B978-0-08-

338 045316-3.00002-8.

339 [12] A.J.D. Silvestre, A. Gandini, Chapter 4 - Rosin: Major Sources, Properties and

340 Applications, in: Elsevier, 2008: pp. 67–88. doi:https://doi.org/10.1016/B978-0-08-

341 045316-3.00004-1.

342 [13] M. Ghanmi, A. El Abid, A. Chaouch, A. Aafi, M. Aberchane, A. El Alami, A. Farah,

343 Étude du rendement et de la composition de l'essence de térébenthine du Maroc: Cas

344 du Pin maritime (Pinus pinaster) et du Pin d'Alep (Pinus halepensis), Acta Bot. Gall.

345 152 (2005) 3–10. doi:10.1080/12538078.2005.10515450.

346 [14] T.L. Eberhardt, P.M. Sheridan, J.M. Mahfouz, Monoterpene persistence in the

347 sapwood and heartwood of longleaf pine stumps: Assessment of differences in

348 composition and stability under field conditions, Can. J. For. Res. 39 (2009) 1357–

349 1365. doi:10.1139/X09-063.

350 [15] H. Wang, B. Liu, X. Liu, J. Zhang, M. Xian, Synthesis of biobased epoxy and curing

351 agents using rosin and the study of cure reactions, Green Chem. 10 (2008) 1190–1196.

352 doi:10.1039/b803295e.

353 [16] Fao, Gum naval stores: turpentine and rosin from pine resin, 1995.

354 [17] M. Ghanmi, B. Satrani, A. Aafi, R. Ismail, A. Farah, A. Chaouch, R. Ismaili,

355 Évaluation de la qualité de la colophane du pin maritime (Pinus pinaster) et du pin

356 d'Alep (Pinus halepensis) du Maroc Évaluation de la qualité de la colophane du pin

357 maritime (Pinus pinas-ter) et du pin d'Alep (Pinus halepensis) du Maroc, Acta Bot.

358 Gall. 156 (2009) 427–435. doi:10.1080/12538078.2009.10516168.

359 [18] M.J. Lombardero, J. Pereira-Espinel, M.P. Ayres, Foliar terpene chemistry of Pinus

360 pinaster and P. radiata responds differently to Methyl Jasmonate and feeding by larvae

361 of the pine processionary moth, For. Ecol. Manage. 310 (2013) 935–943.

362   doi:https://doi.org/10.1016/j.foreco.2013.09.048.

363   [19] İ. Tümen, E.K. Akkol, H. Taştan, I. Süntar, M. Kurtca, Research on the antioxidant,

364   wound healing, and anti-inflammatory activities and the phytochemical composition of

365   maritime pine (Pinus pinaster Ait), J. Ethnopharmacol. 211 (2018) 235–246.

366   doi:https://doi.org/10.1016/j.jep.2017.09.009.

367   [20] E. Gonçalves, A.C. Figueiredo, J.G. Barroso, J. Henriques, E. Sousa, L. Bonifácio,

368   Effect of Monochamus galloprovincialis feeding on Pinus pinaster and Pinus pinea,

369   oleoresin and insect volatiles, Phytochemistry. 169 (2020) 112159.

370   doi:https://doi.org/10.1016/j.phytochem.2019.112159.

371   [21] M. Lai, L. Zhang, L. Lei, S. Liu, T. Jia, M. Yi, Inheritance of resin yield and main resin

372   components in Pinus elliottii Engelm. at three locations in southern China, Ind. Crops

373   Prod. 144 (2020) 112065. doi:https://doi.org/10.1016/j.indcrop.2019.112065.

374   [22] B.L. Lee, D. Koh, H.Y. Ong, C.N. Ong, High-performance liquid chromatographic

375   determination of dehydroabietic and abietic acids in traditional Chinese medications,

376   in: J. Chromatogr. A, 1997: pp. 221–226. doi:10.1016/S0021-9673(96)00901-6.

377   [23] P.J. Kersten, B.J. Kopper, K.F. Raffa, B.L. Illman, Rapid analysis of abietanes in

378   conifers, J. Chem. Ecol. 32 (2006) 2679–2685. doi:10.1007/s10886-006-9191-z.

379   [24] B.K. Via, C. Zhou, G. Acquah, W. Jiang, L. Eckhardt, Near infrared spectroscopy

380   calibration for wood chemistry: Which chemometric technique is best for prediction

381   and interpretation?, Sensors (Switzerland). 14 (2014) 13532–13547.

382   doi:10.3390/s140813532.

383   [25] J. Sandak, A. Sandak, R. Meder, Assessing trees, wood and derived products with near

384   infrared spectroscopy: Hints and tips, in: J. Near Infrared Spectrosc., IM Publications

385   LLP, 2016: pp. 485–505. doi:10.1255/jnirs.1255.

386   [26] R.A. Crocombe, Portable Spectroscopy., Appl. Spectrosc. 72 (2018) 1701–1751.

387   doi:10.1177/0003702818809719.

388   [27] A.V. Morillas, J. Gooch, N. Frascione, Feasibility of a handheld near infrared device

389   for the qualitative analysis of bloodstains, Talanta. 184 (2018) 1–6.

390   doi:10.1016/j.talanta.2018.02.110.

391   [28] V. Wiedemair, D. Langore, R. Garsleitner, K. Dillinger, C. Huck, V. Wiedemair, D.

392   Langore, R. Garsleitner, K. Dillinger, C. Huck, Investigations into the Performance of

393   a Novel Pocket-Sized Near-Infrared Spectrometer for Cheese Analysis, Molecules. 24

394   (2019) 428. doi:10.3390/molecules24030428.

395   [29] B.K. Wilson, H. Kaur, E.L. Allan, A. Lozama, D. Bell, A New Handheld Device for

396   the Detection of Falsified Medicines: Demonstration on Falsified Artemisinin-Based

397   Therapies from the Field, Am. J. Trop. Med. Hyg. 96 (2017) 1117–1123.

398   doi:10.4269/ajtmh.16-0904.

399   [30] F. Kosmowski, T. Worku, Evaluation of a miniaturized NIR spectrometer for cultivar

400   identification: The case of barley, chickpea and sorghum in Ethiopia, PLoS One. 13

401   (2018) e0193620. doi:10.1371/journal.pone.0193620.

402   [31] V. Wiedemair, C.W. Huck, Evaluation of the performance of three hand-held near-

403   infrared spectrometer through investigation of total antioxidant capacity in gluten-free

404   grains, Talanta. 189 (2018) 233–240. doi:10.1016/j.talanta.2018.06.056.

405   [32] M. Li, Z. Qian, B. Shi, J. Medlicott, A. East, Evaluating the performance of a consumer

406   scale SCiO^{TM} molecular sensor to predict quality of horticultural products, Postharvest

407   Biol. Technol. 145 (2018) 183–192. doi:10.1016/j.postharvbio.2018.07.009.

408   [33] G. Drive, A. Suite, C. Stream, C.M. Spectrometry, R.P. Adams, Identification of

409   Essential Oil Components by Gas Review : Identification of Essential Oil Components

410   by Gas Chromatography / Mass Spectrometry, (2005).

411   [34] A. D6730-19, Standard Test Method for Determination of Individual Components in

412   Spark Ignition Engine Fuels by 100-Metre Capillary (with Precolumn) High-

413   Resolution Gas Chromatography, West Conshohocken, 2019.

414   https://www.astm.org/Standards/D6730.htm (accessed December 27, 2019).

415 [35] T. Cabaret, Y. Gardere, M. Frances, L. Leroyer, B. Charrier, Measuring interactions

416   between rosin and turpentine during the drying process for a better understanding of

417   exudation in maritime pine wood used as outdoor siding, Ind. Crops Prod. 130 (2019)

418   325–331. doi:10.1016/j.indcrop.2018.12.080.

419 [36] T. Cabaret, F. Mariet, K. Li, L. Leroyer, B. Charrier, High temperature drying effect

420   against resin exudation for maritime pine wood used as outdoor siding, Eur. J. Wood

421   Wood Prod. 77 (2019) 673–680. doi:10.1007/s00107-019-01425-8.

422 [37] S. Rosen, D. Goldring, D. Sharon, U. Kinrot, I. Bakish, N. Ittai, Spectrometry system

423   applications, 2017.

424 [38] P.P. Subedi, K.B. Walsh, Assessment of avocado fruit dry matter content using

425   portable near infrared spectroscopy: Method and instrumentation optimisation,

426   Postharvest Biol. Technol. 161 (2020) 111078.

427   doi:https://doi.org/10.1016/j.postharvbio.2019.111078.

428 [39] M. Zeaiter, D. Rutledge, Preprocessing Methods, in: Compr. Chemom., Elsevier, 2009:

429   pp. 121–231. doi:10.1016/B978-044452701-1.00074-0.

430 [40] Å. Rinnan, F. van den Berg, S.B. Engelsen, Review of the most common pre-

431   processing techniques for near-infrared spectra, TrAC Trends Anal. Chem. 28 (2009)

432   1201–1222. doi:10.1016/j.trac.2009.07.007.

433 [41] R.J. Barnes, M.S. Dhanoa, S.J. Lister, Standard normal variate transformation and de-

434   trending of near-infrared diffuse reflectance spectra, Appl. Spectrosc. 43 (1989) 772–

435   777. doi:10.1366/0003702894202201.

436 [42] I.S. Helland, T. Næs, T. Isaksson, Related versions of the multiplicative scatter

437   correction method for preprocessing spectroscopic data, Chemom. Intell. Lab. Syst. 29

438   (1995) 233–241. doi:10.1016/0169-7439(95)80098-T.

439   [43] H. Mark, J. Workman, Chapter 57 - Derivatives in Spectroscopy: Part 3—Computing

440   the Derivative (the Savitzky-Golay Method)☆, in: H. Mark, J.B.T.-C. in S. (Second E.

441   Workman   (Eds.),   Academic   Press,   2018:   pp.   371–381.

442   doi:https://doi.org/10.1016/B978-0-12-805309-6.00057-X.

443   [44] J.-R. Bouveresse, Maalouly, Jaillais, Sélection d'échantillons représentatifs par des

444   méthodes chimiométriques. Application à des modèles d'étalonnage, Spectra Anal. 33

445   (2004).

446   [45] R.D. Snee, Validation of Regression Models: Methods and Examples, Technometrics.

447   (1977). doi:10.1080/00401706.1977.10489581.

448   [46] H. Wold, Estimation of Principal Components and Related Models by Iterative Least

449   squares, Acad. Press. New York. (1966) 391–420. doi:[1] E. Devices, D.E. Mccumber,

450   A.G. Chynoweth, A.G. Foyt, B. Elschner, M. Schlaak, References 1., 24 (1967) 10–12.

451   [47] S. Wold, H. Martens, H. Wold, The multivariate calibration problem in chemistry

452   solved by the PLS method, in: Springer, Berlin, Heidelberg, 1983: pp. 286–293.

453   doi:10.1007/BFb0062108.

454   [48] P. Williams, The *RPD* Statistic: A Tutorial Note, NIR News. 25 (2014) 22–26.

455   doi:10.1255/nirn.1419.

456   [49] C. Cordella, D. Bertrand, SAISIR: A new general chemometric toolbox, TrAC - Trends

457   Anal. Chem. 54 (2014) 75–82. doi:10.1016/j.trac.2013.10.009.

458   [50] C. Arrabal, M. Cortijo, B.F. de Simón, M.C. García Vallejo, E. Cadahía,

459   Differentiation among five Spanish Pinus pinaster provenances based on its oleoresin

460   terpenic   composition,   Biochem.   Syst.   Ecol.   33   (2005)   1007–1016.

461   doi:https://doi.org/10.1016/j.bse.2005.03.003.

462   [51]   Y. Ozaki, Near-infrared spectroscopy-its versatility in analytical chemistry, Anal. Sci.
463   28 (2012) 545–563. doi:10.2116/analsci.28.545.

464   [52]   V. Wiedemair, C.W. Huck, Evaluation of the performance of three hand-held near-
465   infrared spectrometer through investigation of total antioxidant capacity in gluten-free
466   grains, Talanta. 189 (2018) 233–240. doi:10.1016/j.talanta.2018.06.056.

467   [53]   M. Schwanninger, J.C. Rodrigues, K. Fackler, A review of band assignments in near
468   infrared spectra of wood and wood components, J. Near Infrared Spectrosc. 19 (2011)
469   287–308. doi:10.1255/jnirs.955.

470   [54]   L. Workman, J. Weyer, Practical Guide and Spectral Atlas for Interpretive Near-
471   Infrared Spectroscopy, CRC Press, 2012. doi:10.1201/b11894.

472   [55]   M. Blanco, I. Villarroya, NIR spectroscopy: A rapid-response analytical tool, TrAC -
473   Trends Anal. Chem. 21 (2002) 240–250. doi:10.1016/S0165-9936(02)00404-1.

474   [56]   Y.B. Ma, K.S. Babu, J.K. Amamcharla, Prediction of total protein and intact casein in
475   cheddar cheese using a low-cost handheld short-wave near-infrared spectrometer, Lwt.
476   (2019). doi:10.1016/j.lwt.2019.04.039.

477

Figure 1 Detailed overview of the Multivariate Data Analysis.
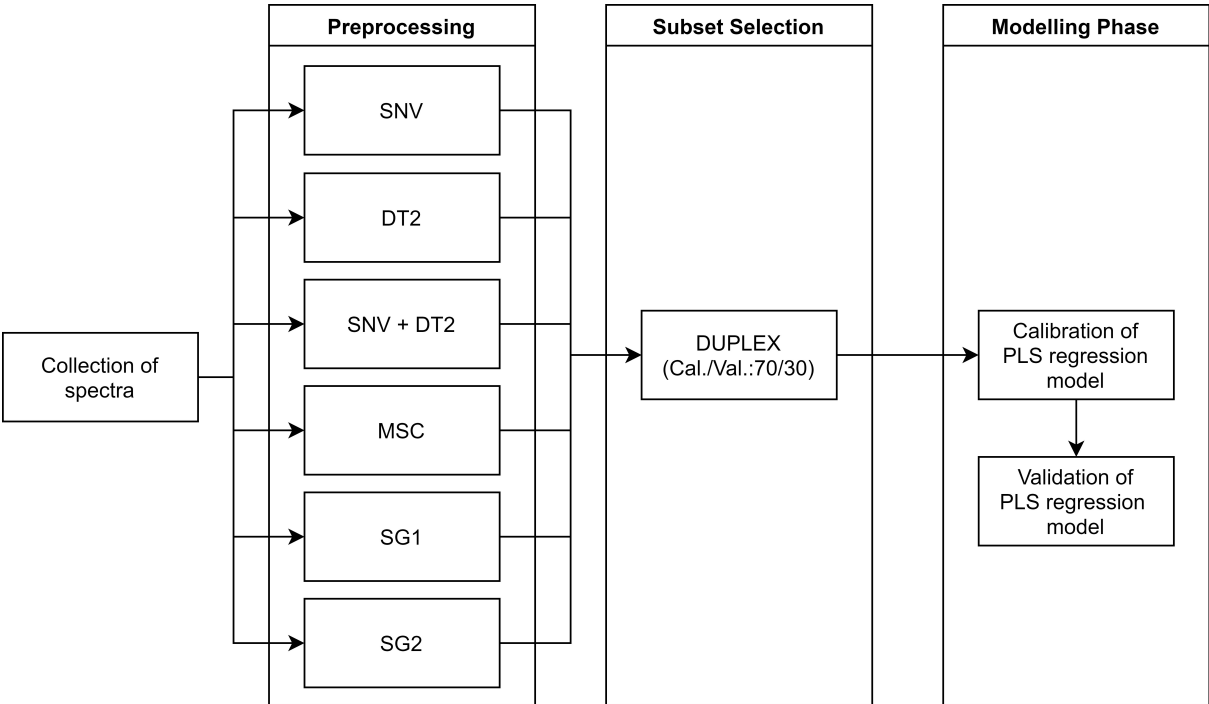
Figure 2 Different preprocessing algorithms were applied to the raw spectra acquired with *SCiO* (*Consumer Physics*, Israel). (a) Raw spectra; (b) SNV preprocessed spectra; (c) DT2 preprocessed spectra; (d) SNV + DT2 preprocessed spectra; (e) MSC preprocessed spectra; (f) SG1 preprocessed spectra; (g) SG2 preprocessed spectra.
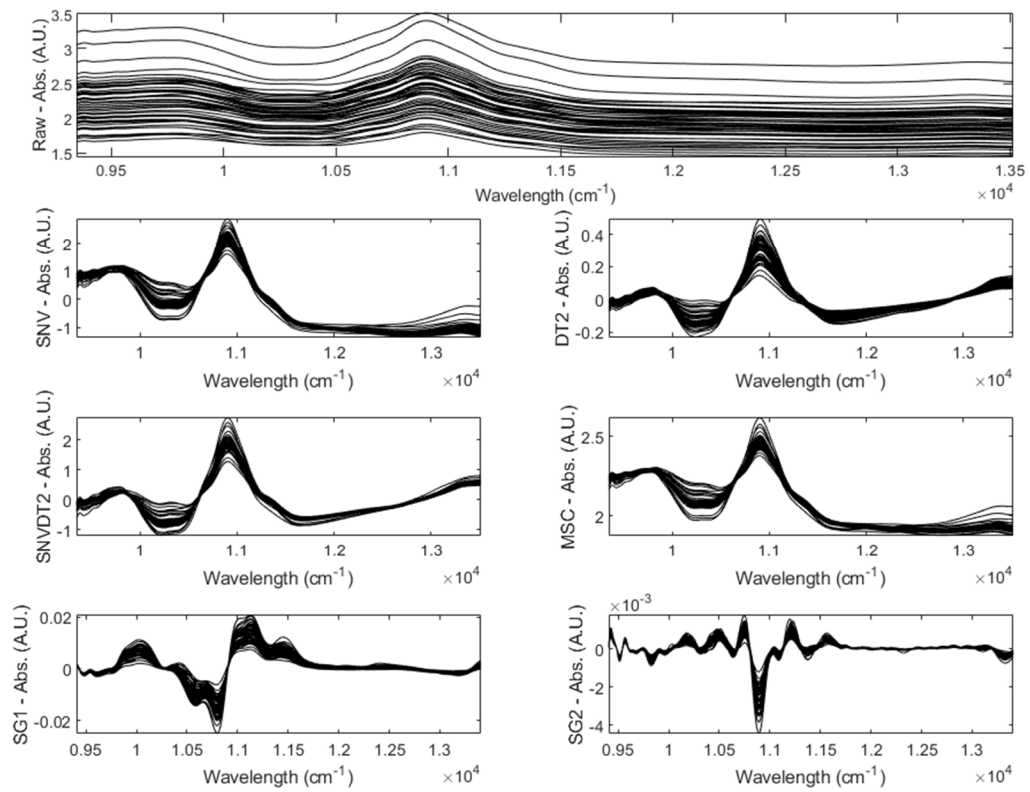
Figure 3 Different preprocessing algorithms were applied to the raw spectra acquired with *MultiPurpose Analyzer I* (*Bruker*, USA). (a) Raw spectra; (b) SNV preprocessed spectra; (c) DT2 preprocessed spectra; (d) SNV + DT2 preprocessed spectra; (e) MSC preprocessed spectra; (f) SG1 preprocessed spectra; (g) SG2 preprocessed spectra.
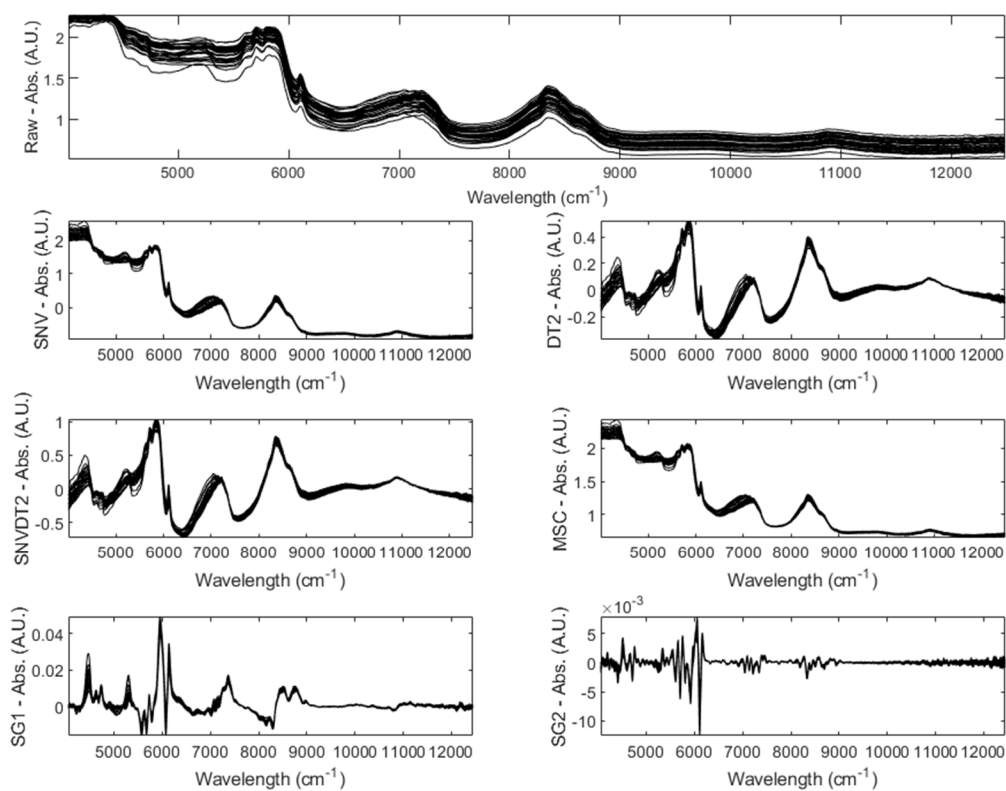
Table 1 Values of the parameters of the analyzed samples of maritime pine (*Pinus pinaster*): main chemical components of the turpentine and rosin fractions, and proportion of the turpentine fraction.

	Parameters	Number of samples	Minimum (%)	Maximum (%)	Mean (%)	Standard deviation (%)
Turpentine Chemical Composition	α-pinene		44.05	84.37	66.16	9.01
	β-pinene		3.24	37.47	18.47	8.45
	Myrcene or/and δ-3 carene	94	0.04	0.52	0.28	0.11
	Limonene		0.88	6.12	4.08	0.68
	ɣ-terpinene		0.64	2.19	1.42	0.30
Rosin Chemical Composition	Levopimaric acid	49	49.66	75.25	62.10	5.93
	Abietic and Neoabietic acids		24.75	50.34	37.90	5.93
% Turpentine	% Turpentine	112	15	52.8	34.25	6.58

Table 2 Band assignments for the chemical components of maritime pine (*Pinus Pinaster*) resin.

Device	Wavenumber (cm^{-1})	(nm)	Functional group	Possible band assignments for: Turpentine constituents	Rosin constituents
MultiPurpose Analyzer I	10891	918	CH methylene (CH_2)		
	9889	1011	OH from tertiary alcohols $(C-OH)$		
	8662	1154	$C=O$ from Carbonyl $(C=O)$		
	7211	1387	CH methyl associated with aromatic $(Ar-CH_3)$		
	6911	1447	CH aromatic (Ar)		
	6101	1639	CH from vinyl group as $(CH_2=CH-)$		
	5816	1719	CH methyl (CH_3)		
	5708	1752	CH methylene (CH_2)		
	5600	1786	CH methylene (CH_2)		
	5222	1915	$C=O$ (carbonyl) from acid $(C=OOH)$		
	4535	2205	CH aromatic (Aryl)		
	4420	2262	CH (CH Bending)		
SCiO	11074	903	CH methylene (CH_2)		
	10787	927	CH methylene (CH_2)		
	10449	957	OH Alkyl Alcohols $(R-C-OH)$		
	9843	1016	OH from tertiary alcohols as $(-C-OH)$		
	9443	1059	OH with hydrogen bonding $(R-C-OH)$		

Table 3 Statistics of Partial Least Squares (PLS) regression models.

	Preprocessing	SCiO (Consumer Physics, Israel)								MultiPurpose Analyzer I (Bruker, USA)							
		LVs	R^2_{Cal}	R^2_{CV}	R^2_{Val}	RMSEC	RMSECV	RMSEP	RPD	LVs	R^2_{Cal}	R^2_{CV}	R^2_{Val}	RMSEC	RMSECV	RMSEP	RPD
α-pinene	RAW	9	0,87	0,83	0,46	3,33	3,71	5,57	1,23	5	0,86	0,87	0,81	3,28	3,25	3,81	2,33
	SNV	10	0,90	0,86	0,64	2,71	3,33	6,57	1,53	4	0,90	0,89	0,89	2,88	2,92	3,10	2,87
	DT2	10	0,93	0,92	0,85	2,36	2,57	4,13	2,28	6	0,94	0,92	0,94	1,99	2,54	2,85	3,63
	SNV + DT2	12	0,91	0,92	0,89	2,40	2,57	3,49	3,09	6	0,94	0,94	0,92	2,10	2,13	2,79	3,42
	MSC	9	0,86	0,86	0,81	3,31	3,38	3,96	2,35	4	0,91	0,90	0,91	2,79	2,87	3,03	2,82
	SG1	8	0,95	0,92	0,76	1,95	2,47	4,56	1,93	**6**	**0,97**	**0,97**	**0,95**	**1,53**	**1,66**	**2,00**	**4,70**
	SG2	**5**	**0,93**	**0,92**	**0,91**	**2,26**	**2,47**	**3,24**	**3,16**	4	0,96	0,95	0,94	1,72	1,91	2,44	4,16
β-pinene	RAW	10	0,92	0,87	0,47	2,35	3,07	5,49	1,35	10	0,96	0,96	0,94	1,61	1,78	2,19	3,69
	SNV	10	0,90	0,88	0,52	2,70	2,95	7,63	1,11	9	0,97	0,96	0,94	1,47	1,59	2,01	4,12
	DT2	8	0,89	0,90	0,85	2,71	2,70	3,64	2,52	5	0,88	0,88	0,91	2,71	2,90	3,13	3,11
	SNV + DT2	9	0,90	0,89	0,86	2,39	2,75	3,99	2,54	7	0,96	0,94	0,93	1,69	2,08	2,38	3,83
	MSC	9	0,89	0,87	0,84	2,58	2,99	3,88	2,42	8	0,96	0,95	0,95	1,62	1,91	1,97	4,45
	SG1	10	0,96	0,95	0,85	1,62	1,91	3,29	2,66	8	0,99	0,98	0,89	0,78	1,13	2,99	3,09
	SG2	**4**	**0,93**	**0,92**	**0,87**	**2,16**	**2,45**	**3,26**	**2,82**	**4**	**0,96**	**0,96**	**0,96**	**1,66**	**1,79**	**1,91**	**4,96**
Levopimaric acid	RAW	6	0,84	0,86	0,81	3,77	4,27	3,45	1,98	9	0,92	0,92	0,92	2,48	2,67	2,60	3,42
	SNV	6	0,80	0,84	0,85	3,86	4,22	3,99	2,51	7	0,93	0,93	0,94	2,38	2,76	2,29	3,87
	DT2	5	0,82	0,84	0,87	3,71	4,25	3,70	2,55	9	0,95	0,94	0,94	1,95	2,15	2,72	3,81
	SNV + DT2	4	0,76	0,78	0,88	4,01	4,09	3,77	2,85	5	0,89	0,90	0,83	2,90	2,88	4,26	2,24
	MSC	**6**	**0,78**	**0,81**	**0,89**	**4,09**	**4,66**	**3,01**	**3,09**	6	0,90	0,90	0,95	2,89	2,80	2,27	3,75
	SG1	6	0,89	0,93	0,79	2,89	3,04	4,14	2,13	**6**	**0,93**	**0,93**	**0,94**	**2,43**	**2,65**	**2,38**	**3,95**
	SG2	5	0,85	0,86	0,86	3,26	3,69	3,93	2,60	4	0,90	0,91	0,94	2,69	2,91	2,72	3,72
Abietic and neoabietic acids	RAW	7	0,86	0,91	0,86	3,50	3,61	3,00	2,28	8	0,93	0,93	0,94	2,29	2,59	2,34	3,80
	SNV	6	0,72	0,73	0,59	4,76	5,39	6,63	1,51	**9**	**0,94**	**0,94**	**0,96**	**2,17**	**2,53**	**2,06**	**4,30**
	DT2	**8**	**0,86**	**0,88**	**0,90**	**3,23**	**3,53**	**3,13**	**3,01**	7	0,95	0,95	0,95	1,87	1,98	2,59	3,99
	SNV + DT2	3	0,28	0,29	0,65	7,08	7,44	7,34	1,47	7	0,95	0,96	0,94	2,06	2,18	2,24	4,25
	MSC	7	0,61	0,61	0,82	6,56	6,89	3,98	2,34	8	0,94	0,95	0,95	2,26	2,57	2,17	3,92
	SG1	6	0,91	0,91	0,84	2,67	2,62	3,52	2,51	4	0,90	0,91	0,90	2,88	3,04	2,94	3,19
	SG2	3	0,85	0,86	0,88	3,22	3,78	3,56	2,87	3	0,90	0,90	0,94	2,66	2,96	2,64	3,83
% Turpentine	RAW	7	0,89	0,91	0,79	3,09	3,25	3,35	2,04	5	0,91	0,92	0,90	2,63	2,58	2,82	3,16
	SNV	6	0,85	0,85	0,68	3,37	3,92	6,87	1,46	6	0,89	0,90	0,87	2,98	3,11	3,24	2,74
	DT2	8	0,88	0,90	0,90	3,07	3,34	3,17	2,98	7	0,92	0,92	0,90	2,42	2,72	3,42	3,02
	SNV + DT2	**5**	**0,78**	**0,82**	**0,89**	**3,86**	**4,06**	**3,56**	**3,03**	6	0,90	0,91	0,88	2,78	3,04	3,30	2,89
	MSC	7	0,73	0,79	0,78	4,98	5,25	4,67	1,99	6	0,89	0,91	0,92	3,09	3,42	2,96	2,88
	SG1	4	0,90	0,92	0,83	2,87	3,29	3,56	2,48	5	0,89	0,91	0,91	3,03	3,20	2,73	3,44
	SG2	5	0,87	0,88	0,89	3,05	3,28	3,42	2,99	**4**	**0,89**	**0,91**	**0,92**	**2,86**	**3,07**	**2,94**	**3,45**

Graphical Abstract

Samples: sealed tank containing resin from *Pinus pinaster* tapping

Chemical analysis

- GC-FID
  - α-pinene, β-pinene
- HPLC-DAD
  - Levopimaric, abietic, and neoabietic acids

Spectroscopy

- *SCiO molecular sensor* (Consumer Physics, Israel)
  - Spectral range: 740 to 1070 nm
- *MultiPurpose Analyzer I* (Bruker, USA)
  - Spectral range: 780 to 2400 nm

Modelling phase

Preprocessing

Subset selection

Calibration (Partial Least Squares regression)

Validation of PLS regression model

Sucessful Predictive Models